SPIN 6 (1) (2024) 27-33

SPIN
JURNAL KIMIA & PENDIDIKAN KIMIA
https://journal.uinmataram.ac.id/index.php/spin

# GREEN SYNTHESIS OF TITANIUM DIOXIDE USING BIANCAEA SAPPAN EXTRACT AS REDUCTORS

**Risya Sasri[1*], A. Ifriany Harun[2]**

[1]Program Studi Kimia, Fakultas Matematika dan Ilmu Pengetahuan Alam Universitas Tanjungpura.
[2]Program Studi Pendidikan Kimia, Fakultas Keguruan dan Ilmu Pendidikan Universitas Tanjungpura, Pontianak, 78124.

**DOI: 10.20414/spin.v6i1.8903**

History Article
Accepted:
Nov 24, 2023
reviewed:
May 17, 2024
Published:
July 13, 2024

Kata Kunci:
Kayu secang, Síntesis hijau, $TiO_2$

Keywords:
Green synthesis, *Sappan wood.*, $TiO_2$



**ABSTRAK**

Telah dilakukan sintesis $TiO_2$ berbasis *green chemistry* melalui reduksi prekursor titanium isopropoksida oleh ekstrak kayu secang (Biancaea sappan *L.*) sebagai bioreduktor. Tujuan penelitian ini adalah untuk mengkaji karakteristik material nanokomposit $TiO_2$ berdasarkan hasil analisis dengan difraksi sinar- X (XRD) dan *diffuse reflectance* UV-Vis. $TiO_2$ disintesis melalui metode sol gel menggunakan larutan ekstrak kayu secang dalam pelarut etanol. Proses kristalisasi dilakukan dengan kalsinasi pada suhu $40^0$C selama 2 jam. Karakteristik $TiO_2$ hasil sintesis hijau memperlihatkan sudut difraksi, jarak antar bidang dan bidang kristal yang bersesuaian dengan $TiO_2$ standar dengan indikasi terbentuknya nanopartikel $TiO_2$ berdasarkan analisis XRD. Nilai Energi celah pita ($E_{gap}$) $TiO_2$ sintesis sebesar 2,46 eV yang diperoleh dari analisis DR UV-Vis dengan persamaan Kubelka Munk. Berdasarkan data yang diperoleh, maka $TiO_2$ nanopartikel dapat disintesis melalui sintesis hijau (*green chemistry*) menggunakan titanium tetraisopropoksida sebagai prekursor Ti yang direduksi dengan ekstrak kayu secang dalam pelarut etanol.

**ABSTRACT**

The synthesis of $TiO_2$ through green chemistry principles was conducted by reducing titanium isopropoxide precursors using sappan (*Biancaea sappan L)* wood extract as a reductant. The research aimed to investigate the characteristics of $TiO_2$ nanocomposite materials through analysis using X-ray diffraction (XRD) and UV-Vis diffuse reflectance. $TiO_2$ was synthesized using the sol-gel method with a solution of sappan wood extract in ethanol solvent. The crystallization process involved calcination at 400°C for 2 hours. The characteristics of $TiO_2$ produced through green synthesis exhibited diffraction angles, distances between planes, and crystal planes corresponding to standard $TiO_2$, indicating the formation of $TiO_2$ nanoparticles based on XRD analysis. The Gap Energy ($E_{gap}$) value of synthetic $TiO_2$ was determined to be 2.46 eV through DR UV-Vis analysis using the Kubelka-Munk equation. Based on the obtained data, it can be concluded that $TiO_2$ nanoparticles can be successfully synthesized via green synthesis (*green chemistry*) using titanium tetraisopropoxide as a Ti precursor, which is then reduced with sappan wood extract in ethanol solvent.

**How to Cite**

Sasri, R., & Harun, A. I., (2024). Green Synthesis of Titanium Dioxide Using Biancaea Sappan Extract as Reductors. *SPIN-Jurnal Kimia & Pendidikan Kimia*. 6(1). 27-33.

*Correspondence Author:
Email: risya@untan.ac.id

**p-ISSN: 2580-2623**
**e-ISSN: 2745-6854**

## INTRODUCTION

In the last few decades, research on green synthesis has experienced massive development. This includes sustainable approaches to the synthesis of nanoparticles and nanocomposite materials. Green synthesis techniques will have an impact on a synthesis process that is more environmentally friendly, uses fewer chemicals, and requires cheaper production costs. This supports efforts to harmonize eco-techno-friendliness in people's lives. Green synthesis that is developing, especially in synthesizing nanomaterials, is replacing chemical-reducing agents with plant extracts as reducing agents. This bioreductor can then be used on a large scale with cheaper production costs. Apart from that, the use of plant extracts will reduce the use of chemicals that can be toxic so that they are more environmentally friendly (Wahyuni & AriefiV, 2019).

$TiO_2$ nanoparticles are among the most widely developed materials for several properties and potential uses, such as semiconductors, photocatalysts, smart packaging, storage, and drug delivery. The use of $TiO_2$ Nanoparticles as semiconductors and photocatalysts, in particular, is often associated with the function of $TiO_2$ composites with several metal oxides and organic compounds as smart materials (Sasri et al., 2014).

Aravind et al. (2021) carried out the green synthesis of $TiO_2$ using lily flower extract, which contains alkaloids, coumarins, and flavonoids as reducing agents. The X-ray diffractogram results show that the $TiO_2$ produced has a rutile phase with an average crystal size of 31 – 42 nm. Based on UV-Vis analysis, it was found that the $TiO_2$ absorption was at a wavelength of 385 nm. Ti-O-Ti and Ti-O bond vibrations were confirmed through analysis with infrared spectrophotometry. The shape of the $TiO_2$ material is seen using SEM, which gives an image of a round shape. Apart from that, the results of the photodegradation test stated that the $TiO_2$ resulting from green synthesis provided an efficiency of 92% (Aravind et al., 2021).

Various studies have been carried out to examine green synthesis techniques for $TiO_2$ nanoparticles with metal oxide composites. Belver et al. (2023) carried out green synthesis of CuO-$TiO_2$ nanoparticles to degrade organic pollutants using a weed plant extract reductant with the scientific name Commelina. Bengalensis. The research results reported that the CuO-$TiO_2$ composite has an anatase $TiO_2$ structure based on XRD analysis and is mesoporous in SEM data analysis. Furthermore, organic compound degradation tests stated that the composite could degrade methylene blue dye and the antibiotics sulfisoxazole and ciprofloxacin (Belver et al., 2023).

Wahyuni & Ariefin (2019) synthesized Ag/$TiO_2$ using gambier leaf extract (*Uncarua gambir Roxb*). The synthesis results reported that the material structure was confirmed to be an anatase phase with surface plasmon resonance at 426 nm. The presence of Ag metal oxide in $TiO_2$ can increase the UV-Vis absorption of $TiO_2$ from 407 nm to 438 nm. Next, a degradation test was carried out using the synthetic dye rhodamine B, and the results showed that the photodegradation ability of the Ag/$TiO_2$ synthetic material provided an efficiency of 99% (Wahyuni & AriefiV, 2019).

Bhardwaj & Singh (2021), carried out a green synthesis of Ag-$TiO_2$ nanocomposite using Origanum majoarana leaf extract using the sonication method and studied its biological activity. The results obtained were round-shaped nanocomposites with an average size of 25-50 nm based on SEM-EDX analysis. Furthermore, the results of the synthesis of Ag–$TiO_2$ nanocomposites showed significant antimicrobial activity against Escherichia coli, Bacillus subtilis, and Aspergillus niger compared to $TiO_2$ nanoparticles. Evaluation of the biomimetic synthesized Ag-$TiO_2$ antioxidant also showed strong activity compared to $TiO_2$ nanoparticles and

comparable to standards. Thus, green synthesized Ag-$TiO_2$ nanocomposites provide a promising approach that can meet the requirements of large-scale industrial production with the advantages of low cost, environmental friendliness, and reproducibility (Bhardwaj & Singh, 2021).

The use of sappan wood as a reducing agent in the green synthesis of nanomaterials has also been studied. Sappan wood, known as *Biancaea sappan* L., is a medicinal plant often used in Southeast Asia, including Indonesia. Secang wood is traditionally consumed as an herbal drink to increase endurance, kill bacteria, treat diarrhea, and treat tumors. *Biancaea sappan* L. has a scientific synonym called Caesalpinia sappan L., which contains homoisoflavonoids and phenols such as brazilin (Vardhani, 2019).

Amin & Sutoyo (2022) synthesized silver nanoparticles using the bioreductant secang wood extract. This research report shows that silver nanoparticles were successfully synthesized and had a particle size of 618.1 nm. The maximum absorption of Ag was confirmed to be at a wavelength of 446 nm. Based on the results of the FT-IR analysis, it is stated that OH vibration is a hydroxyl functional group that detects the formation of silver nanoparticles. Taking images via SEM also confirmed that silver nanoparticles were present in agglomerations of varying sizes (Amin & Sutoyo, 2022.).

Based on the review of various related studies above, it is interesting to carry out further research on the synthesis of $TiO_2$ nanocomposites with copper metal oxide using the bioreductant sappan wood extract. In this research, green synthesis of $TiO_2$ nanocomposites with CuO metal oxide will be carried out using sappan wood extract as a reducing agent. The resulting nanocomposites will be studied for their material characteristics using XRD and SEM analysis. UV-Vis absorption characteristics will also be studied and continued with electron transition characteristics in band gap energy. In this way, an in-depth study of the material and electronic characteristics of $TiO_2$/Cu nanocomposites with sappan wood extract as a reductant will be obtained.

## METHODS

### Materials

The materials used in this research include Titanium tetraisopropoxide, TTIP (Sigma-Aldrich), Ethanol (Merck), Sappan wood, and Aquades.

### Tools

The tools used in this research include a set of glass equipment such as a beaker, Erlenmenyer, volume pipette, stirring rod, hot plate stirrer, magnetic stirrer, oven (ESCO/OFA1108), digital scales, and furnace (Naberthem/L9/11).

### Sappan wood extraction (Amin & Sutoyo, 2022).

The dried pieces of sappan wood are then macerated with ethanol solvent. 500 g of sappan wood was added with 1L of ethanol and macerated. The maceration solution was filtered using a Buchner funnel to extract ethanol from sappan wood. The combined macerated extract solvent was evaporated using a rotary evaporator to obtain a concentrated ethanol extract of sappan wood. The extract was dried for 8 hours using a freeze dryer to obtain a dry ethanol extract of sappan wood.

### Green synthesis of $TiO_2$ (Bhardwaj & Singh, 2021)

A total of 0.1 M TTIP was added to 15 mL of ethanol and stirred for 10 minutes. 25 ml of sappan wood extract was added and stirred with a stirrer for 1 hour at 200 rpm with a reaction temperature of 50°C (sample A) and room temperature (sample B). Next, it was filtered and dried in an oven at a temperature of 80°C for 24 hours. The next stage is the calcination process of composite nanoparticles using a furnace at a temperature of 400°C for 2 hours. XRD analysis was performed at long angles to confirm the formation of nanoparticles. UV absorption analysis is carried out by examining the absorption and reflectance

characteristics to determine the UV absorption wavelength and electronic transition to obtain the band gap energy of the composite nanoparticle.

## RESULT AND DISCUSSION

Structural analysis of the synthesized $TiO_2$ was carried out based on characterization using X-ray diffraction (XRD). The diffractogram results were compared with standard $TiO_2$ anatase phase data with reference code 01-076-3179. Figure 1 presents the X-ray diffractogram.

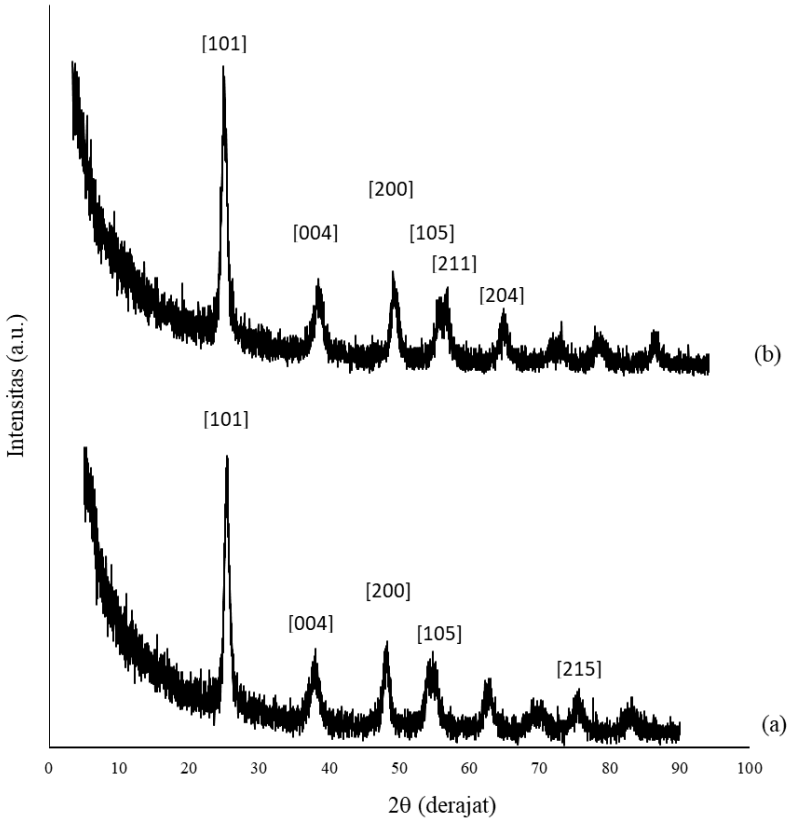


**Figure 1. X-ray diffractogram of $TiO_2$ synthesized from sample A (a) and sample (B)**

Table 1 presents the angular diffraction interpretation data for sample A based on the resulting diffractogram, while the angular interpretation of sample B is presented in Table 3. XRD measurements were carried out at an angle of 5.0084 - 89.9744 [°2Th.] with an X-ray wavelength of 1.54 Å. In Sample A, the intensity was found at an angle of 5.39250, while in Sample B, it was not found. The presence of an angle below 100 usually indicates that there are crystals with mesopore size, which are generally detected at small diffraction angles. The peak intensity at this small diffraction angle can be a characteristic of the formation of $TiO_2$ nanoparticles. However, this hypothesis must be believed by carrying out further analysis in the form of the size of the synthesized $TiO_2$ particles and photographs of their morphology.

Interpretation of the diffractogram data for samples A and B shows similar patterns at the 6 highest intensities listed in the standard $TiO_2$ data with reference code 01-076-3179. The detailed comparison of the diffraction angles is shown in Table 1. Based on the comparison of the diffraction angles and the resulting peak intensities, it can be seen that the trend of the diffraction peaks between sample A and sample B is characteristic and corresponds to the standard $TiO_2$ diffraction angle, especially at an angle of 25.16°, 46.89°, and 53.13°. Abu-Dalo et al. (2019) synthesized $TiO_2$ Nanoparticles (NPs) using a reductant from pomegranate seed extract. The structural characteristics of $TiO_2$ NPs based on XRD data indicate the presence

of a main diffraction peak at 2θ value of 25.20°, 37.80°, 48.04°, 53.89°, 62.68° and 75.1° corresponding to the indexed crystal planes (101), (004), (200), (105), (211), and (204), respectively. The main peaks of $TiO_2$ NPS are confirmed at angles of 25,20° and 48,04° and have an anatase phase (Abu-Dalo et al., 2019). Maurya et al. (2019) also conducted a study on the synthesis of $TiO_2$ using green synthesis. XRD data shows that the appearance of a sharp peak at 2θ 25.30°, 37.80°, 48.10°, 53.90°, 55.10°, 62.70°, 68.80°, 70.30°, and 75.10° represent the crystal plane indices (101), (004), (200), (105), (211), (204), (116), (215) and (303) and confirm the formation of $TiO_2$ highly crystalline synthesis in pure anatase (Maurya et al., 2019).

From samples A and B, it was found that the diffraction angle most similar to standard $TiO_2$ was that shown in sample B. Almost all peaks in sample B showed the same diffraction angle as the standard. The intensity character of the peaks diffracted at angles corresponding to the standard indicates that the material character is expected to be the same. Thus, based on XRD data, it can be concluded that the synthesized material is confirmed as $TiO_2$.

**Table 1. Comparison Data of Diffraction Angles for Samples A and B with Standard $TiO_2$ Diffractogram Reference 01-076-3179 Based on the 6 highest intensities**

| Standard | | Sample A | | Sample B | |
|---|---|---|---|---|---|
| **Angle 2θ(⁰)** | **Intensity (%)** | **Angle 2θ(⁰)** | **Intensity (%)** | **Angle 2θ(⁰)** | **Intensity (%)** |
| 25,1640 | 100 | 25,4097 | 100 | 25,1640 | 100 |
| 46,892 | 24,4 | 5,3925 | 36,4 | 47,9030 | 28,29 |
| 37,377 | 20,6 | 48,1576 | 31,67 | 37,7323 | 20,30 |
| 53,132 | 13,3 | 54,0297 | 22,43 | 53,9782 | 19,16 |
| 53,744 | 13,0 | 55,2680 | 20,98 | 55,0941 | 19,15 |
| 61,444 | 10,3 | 62,8695 | 15,98 | 62,8193 | 13,65 |

The peak intensity at the diffraction angle is used to characterize the type of material by comparison with standard data. After the type of material is confirmed, a comparison is made of the distance between the planes and the crystal plane h k l. Table 2 compares the distance values between planes ($d_{spacing}$) and h k l planes in sample A and standard $TiO_2$ and sample B in Table 3.

**Table 2. Comparison of distance values between planes ($d_{spacing}$) and h k l planes in sample A and standard $TiO_2$**

| 2θ (standard) | d (standard) | h k l (standard) | 2θ (sample A) | d (sample A) |
|---|---|---|---|---|
| 25,1640 | 3,59180 | 1 0 1 | 25,4097 | 3,50539 |
| 46,892 | 1,93600 | 2 0 0 | 5,3925 | 16,38863 |
| 37,377 | 2,40400 | 0 0 4 | 48,1576 | 1,88958 |
| 53,132 | 1,72240 | 1 0 5 | 54,0297 | 1,69727 |
| 53,744 | 1,70420 | 2 1 1 | 55,2680 | 1,66214 |
| 61,444 | 1,50780 | 2 0 4 | 62,8695 | 1,47823 |

**Table 3. Comparison of distance values between planes (dspacing) and h k l planes in sample B and standard $TiO_2$**

| 2θ (standard) | d (standard) | h k l (standard) | 2θ (sample B) | d (sample B) |
|---|---|---|---|---|
| 25,1640 | 3,59180 | 1 0 1 | 25,1640 | 3,53906 |
| 46,892 | 1,93600 | 2 0 0 | 47,9030 | 1,89903 |
| 37,377 | 2,40400 | 0 0 4 | 37,7323 | 2,38416 |
| 53,132 | 1,72240 | 1 0 5 | 53,9782 | 1,69877 |
| 53,744 | 1,70420 | 2 1 1 | 55,0941 | 1,66697 |
| 61,444 | 1,50780 | 2 0 4 | 62,8193 | 1,47929 |

Based on the distance between planes or $d_{spacing}$ values, the crystal planes of sample A and sample B have values that correspond to the $TiO_2$ standard. An anomaly occurred in sample A at an angle of 5.39o with a very large $d_{spacing}$ value compared to diffraction at other angles. This is predicted to be due to the influence of the crystal character, which diffracts at small angles. The size of crystal particles diffracted at small angles below 10o may be mesoporous, namely nanoparticles with a size of 50 - 100 nm. This indicates that the $TiO_2$ produced as sample A may have nanoparticle characteristics. Sample A is a $TiO_2$ synthesis involving a reaction temperature of 50°C. Even though peak intensity characteristics and diffraction angles are not exactly the same as the $TiO_2$ standard, sample A shows a nanoparticle pattern. However, a comprehensive particle size analysis must be carried out to ensure the particle size.

$TiO_2$ is a semiconductor material that has photocatalytic activity. $TiO_2$ has a band gap energy ($E_{gap}$) of 3.0 eV in the rutile phase and 3.25 eV in the anata phase. This $E_{gap}$ value is very interesting for $TiO_2$ because some uses of $TiO_2$ in advanced materials engineering are based on modifications to its Egap. Therefore, information regarding the Egap value of the synthesized $TiO_2$ is very important in observing and characterizing the optical properties related to its photocatalytic activity. Egap determination is carried out using data obtained from DR UV-Vis analysis. UV-Vis absorption analysis was carried out at 300 – 700 nm with output data as absorbance and reflectance values.

The reflectance data (%R) also obtained from the DR UV-Vis analysis was then processed using the Kubelka-Munk equation, which plots the Egap value against $(Khv)^2$. K is the Kubelka Munk constant obtained from calculations based on reflectance data.

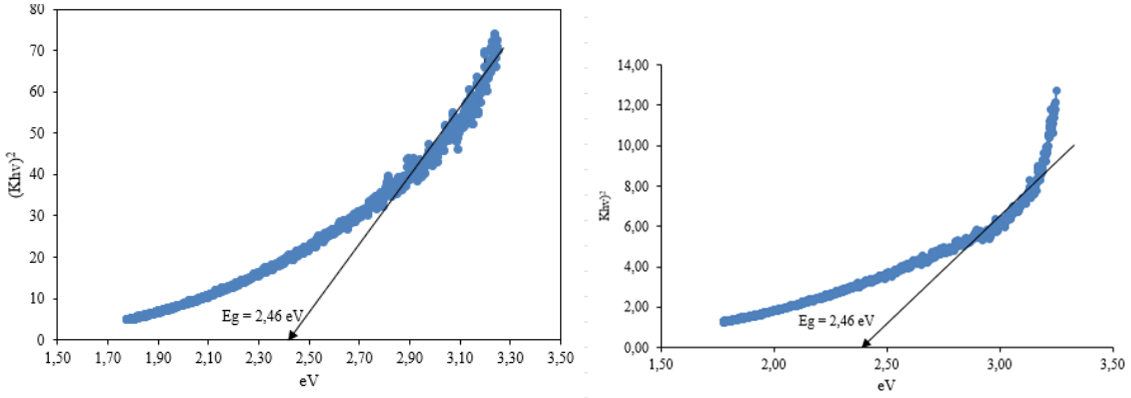


**Figure 2. Band Gap Energy Determination Curve ($E_{gap}$) for Sample A (left) and Band Gap Energy Determination Curve ($E_{gap}$) of Sample B (right)**

Figure 2 shows samples A and B's band gap energy determination curve. The $E_{gap}$ curve for sample A has the line equation y = 83.738x - 206.22, and sample B has the line equation y = 11.316x - 27.856. Based on the line equation, the band gap energy is determined using Tauc's Plot. The band gap energy value is the intersection of the linear extrapolation line with the x-axis or y=0, so by entering the value y=0, you will get the intersection value on the x-axis, expressed as Egap. The Egap produced by both samples shows the same value, 2.46 eV. This Egap value significantly differs from the $E_{gap}$ of rutile and anatas phase $TiO_2$. Maurya et al. (2019) reported that the UV-Vis absorption by green synthetic $TiO_2$ (G-TNP) and conventional $TiO_2$ (TNP) was around 285 nm with a sharp spectrum at 306 nm. The calculation results using Tauc's plot method give an $E_{gap}$ value of 2.9 eV for G-TNP and 3.2 eV for TNP. This shows a significant reduction in Egap between G-TNP and conventional TNP (Maurya et al., 2019). This significant decrease in the Egap value is due to the reducing effect of the sappan wood extract used. Pigments are compounds that easily absorb light due to the presence of chromophore substances, which can influence the differences in the characteristics of the $E_{gap}$ $TiO_2$ produced. Therefore, it is necessary to carry out another analysis to confirm whether

this difference is due to the presence of groups in the sappan wood extract. Synthesis of $TiO_2$ using a reductant from sappan wood extract, the $TiO_2$ produced was able to show the characteristics of $TiO_2$ nanoparticles based on the results of XRD analysis.

## CONCLUSION

$TiO_2$ nanoparticles can be synthesized via green synthesis (green chemistry) using titanium tetraisopropoxide as a Ti precursor, which is reduced with sappan wood extract in ethanol solvent.

The characteristics of $TiO_2$ resulting from green synthesis show diffraction angles and distance between planes and crystal planes, which correspond to standard $TiO_2$ with indications of the formation of $TiO_2$ nanoparticles based on XRD analysis. The $E_{gap}$ value of synthetic $TiO_2$ is 2.46 eV, quite significantly different from standard rutile and anatase phase $TiO_2$.

## ACKNOWLEDGMENT

Thank you and high appreciation to the Teacher Training and Education Faculty at Tanjungpura University, Pontianak, under DIPA UNTAN Grant No. SP DIPA-023.17.2.677517/2023, which contributed to this research.

## REFERENCES

Abu-Dalo, M., Jaradat, A., Albiss, B. A., & Al-Rawashdeh, N. A. F. (2019). Green synthesis of $TiO_2$ NPs/pristine pomegranate peel extract nanocomposite and its antimicrobial activity for water disinfection. *Journal of Environmental Chemical Engineering*, 7(5). https://doi.org/10.1016/j.jece.2019.103370

Amin, R. R., & Sutoyo, S. (2022). International Journal of Current Science Research and Review Green Synthesis and Characterization of Silver Nanoparticles Derived from Ethanol Extract of Sappan Wood. https://doi.org/10.47191/ijcsrr/V5-i7-21

Aravind, M., Amalanathan, M., & Mary, M. S. M. (2021). Synthesis of $TiO_2$ nanoparticles by chemical and green synthesis methods and their multifaceted properties. *SN Applied Sciences*, 3(4). https://doi.org/10.1007/s42452-021-04281-5

Belver, C., Bopape, D. A., Mathobela, S., Matinise, N., Motaung, D. E., & Hintsho-Mbita, N. C. (2023). Green Synthesis of CuO-$TiO_2$ Nanoparticles for the Degradation of Organic Pollutants: *Physical, Optical and Electrochemical Properties*. https://doi.org/10.3390/catal

Bhardwaj, D., & Singh, R. (2021). Green biomimetic synthesis of Ag–$TiO_2$ nanocomposite using Origanum majorana leaf extract under sonication and their biological activities. *Bioresources and Bioprocessing*, 8(1). https://doi.org/10.1186/s40643-020-00357-z

Maurya, I. C., Singh, S., Senapati, S., Srivastava, P., & Bahadur, L. (2019). Green synthesis of $TiO_2$ nanoparticles using Bixa orellana seed extract and its application for solar cells. *Solar Energy*, 194, 952–958. https://doi.org/10.1016/j.solener.2019.10.090

Sasri, R., Kartini, I., & Nuryono. (2014). Serat Nano $TiO_2$ Sebagai Fotoanoda Berbasis Zat Warna Ruthenium Kompleks Untuk Sel Surya. Universitas Gadjah Mada.

Vardhani, A. K. (2019). *ICASH-A042* (Issue 4).

Wahyuni, S., & AriefiV, S. (2019). Jurnal Kimia Sains dan Aplikasi Journal of Scientific and Applied Chemistry of Ag / $TiO_2$ Nanocomposite Assisted by Gambier Leaf (Uncaria gambir Roxb) Extract. *Jurnal Kimia Sains Dan Aplikasi*, *22*(6), 250–255. https://doi.org/10.14710/jksa.22.6